Electrodeposition of DLC films on carbon steel from acetic acid solutions

H. Hassannejad[1,‡], F. Bogani[1], M. Boniardi[2], A. Casaroli[2], C. Mele[1] and B. Bozzini*[1]

Introduction

Applying a hard coating to a surface can improve the resistance to wear and environmental degradation for mechanical and tribological applications. In recent years, diamond-like carbon (DLC) films have attracted interest in the mechanical engineering community because of their unique properties and characteristics such as high hardness, high thermal conductivity, high chemical inertness and high corrosion resistance. The deposition of DLC films has been accomplished by a large number of different methods among which the more extensively documented are: chemical vapour deposition (CVD), physical vapour deposition (PVD) and ion-beam laser processing techniques.[1–10] However, these techniques have disadvantages such as requirement of high voltage, high vacuum and therefore high cost. Thus, an alternative simple, scalable and low-cost method for the deposition of DLC films would be very important. Electrodeposition offers us a novel route of synthesis for DLC films; in 1992, for the first time Namba[11] used electrochemical methods to deposit DLC films on silicon substrates. In his study, DLC films have been deposited on silicon substrates from ethanol solutions at temperatures from room to 70°C, by ramping the potential from 0 to −1·2 kV and obtaining current densities growing from 0 to 5 mA cm^{-2}. After this seminal work, the electrolytic method has been successfully employed to deposit DLC films from different organic solvents such as: methanol, ethanol, acetone and DMF.[11–13] Notwithstanding the advantages of the electrochemical approach with respect to the competing physical methods, in these researches, DLC coatings have been deposited at low temperature, but with a high potential difference between the anode and cathode which greatly increases the difficulty of controlling the growth process.

More recently, A.K. Pal *et al.*[4,15] proposed a simple electrodeposition technique using formic acid, acetic acid (CH_3COOH) and deionised water as the electrolyte; electrolysis was carried out with voltage in the range 2·5–30 V, corresponding to current densities between 10^{-3} and 10^{-5} A cm^{-2}. By this method, diamond phase and amorphous carbon films were both formed, as revealed by Raman spectroscopy. This approach, employing both low potential and low temperature, allows a notable simplification of the setup and process control.

As far as the structure of DLC films is concerned, they have been reported to be generally amorphous and homogeneous, but some micro or nano-crystalline inclusions of all carbon forms are typically found in the amorphous matrix. During film deposition, the carbon atoms can combine at the surface to form all possible combinations of sp^1, sp^2, and sp^3 bonds, the trigonal (sp^2) or tetrahedral (sp^3) configurations

[1]Dipartimento di Ingegneria dell'Innovazione, Università del Salento, via Monteroni, 73100 Lecce, Italy
[2]Dipartimento di Meccanica, Politecnico di Milano, via La Masa 1, 20156 Milano, Italy
[‡]Present address: Department of Materials Engineering, Faculty of Engineering, Arak University, Arak, Iran

*Corresponding author, email benedetto.bozzini@unisalento.it

dictating graphitic or diamond structures, respectively. In general, DLC films consist of graphitic clusters linked by sp^2 (p bonding) and sp^3 bonding (s bonding) forming an extended carbon network. The sp^3/sp^2-bonding ratio is the chief parameter determining the microstructure and hence the physical and mechanical properties of DLC films prepared by different techniques.[6,12,14–18]

In the present paper, the authors present and discuss the electrodeposition process at low temperature and low potential on a ferrous substrate, and the mechanical properties as well as the corrosion resistance of the deposits. In order to characterise the mechanical properties of the coated systems, micro-indentation and scratch-testing have been used.

Materials and methods

DLC films were electrodeposited onto carbon steel using a mixture of H_3COOH and deionised water as electrolyte, varying in the concentration range from 1 to 10 vol%. According to Roy *et al.*,[14] acetic acid in water ionises and is transported in the electrolyte under high electric field, according to reaction (1):

$$CH_3COOH \rightarrow CH_3^+ + CO + OH^- \quad (1)$$

The positively charged methyl groups are attracted to the cathode to form diamond-like carbon films through reaction (2).[14]

$$2\,CH_3^+ + 2e^- \rightarrow 2C + 3H_2 \quad (2)$$

The negatively charged hydroxyl groups, in contrast, migrate towards the anode, where they undergo reaction (3).[18]

$$2OH^- \rightarrow O_2 + H_2O + 4e^- \quad (3)$$

The substrates for DLC electrodeposition were 2 cm × 3 cm (6 cm^2) rectangular coupons cut from a 1 mm thick A284 steel slab. For electrodeposition, a cathodically active area of 4 cm^2 was defined by screening with a PTFE frame. High-purity graphite plates (Goodfellow) were employed as the anode. The anode surface area was ten times larger than that of the cathode, in order to achieve an homogeneous current density distribution. Electrodeposition was carried out in a plane-parallel, two-electrode configuration: the graphite anode was fixed at 0·4 cm from the steel sheet, in order to minimise the electrode gap with the available cell configuration. A volume of 0·5 L of fresh electrolyte was used for the electrodeposition of each sample. The process was carried out starting with a bath at room temperature (*ca.* 25°C), but during electrodeposition a strong Joule heating is obtained in the vicinity of the cathode;[19] such thermal effect has been shown to be desirable for both kinetic (Arrhenius-type) and fluid-dynamic reasons (decrease in viscosity).[18]

Prior to electroplating, the substrates were mechanically polished to a mirror surface finish with emery papers and 1 μm Al_2O_3 and then they were treated as follows sequentially: ultrasonically cleaned in acetone for 300 s, washed in distilled water, activated in 10 vol% HCl for 10 s, washed in distilled water again and then immersed immediately in the plating bath. The experiments were performed potentiostatically at cell voltages in the range from −8 to −20 V and chronoamperometric curves were recorded during electrodeposition. After electrodeposition, the samples were simply rinsed with deionised water and dried in an N_2 stream.

The Vickers microhardness of the DLC coating was determined by applying a load of 25 g for 20 s. Substrate contributions in the hardness determination were accounted for with the method described previously, in Sections 2·1–2·3.[20] The type of carbonaceous species contained in the electrodeposited films was analysed by Raman spectroscopy.[10,12,21,22] Raman measurements were performed with a Raman microprobe system (LabRam Jobin-Yvon) equipped with a confocal microscope, CCD detector, holographic notch filter and mapping facilities with micrometric lateral resolution. The excitation line was 632·8 nm from a HeNe laser delivered at the sample point with about 12 mW. A 50 × long-working-distance objective was used. Scratch-testing was performed in order to evaluate the coating adhesion as a function of deposition potential, time and bath composition. Specimens were scratched using a CSM testing machine, mod. MCT/SN 50-0223, with a preload of 1 N, load speed of 12·5 N min^{-1} up to a maximum load of 30 N, according to the ASTM C1624 standard. Normal and tangential loads were recorded during tests. Scratch lines were measured by SEM (Cambridge Stereoscan 360) in order to determine the critical scratch loads and to allow calculation of the coating shear stresses. Coating thickness was estimated with an UVISEL Spectroscopic Ellipsometer with polariser and incidence angles of 60°. Electrochemical impedance spectrometry (EIS) measurements were carried out in a conventional three-electrode cell in a neutral, aerated 0·8 M NaCl solution. with an Amel 5000 programmable potentiostat linked to a Solartron SI 1250 frequency response analyser. The potential modulation was 10 mV peak-to-peak and the frequency span 65 kHz–10 mHz.

Results and discussion

Electrodeposition process

Electrodeposition tests were carried out under the conditions detailed in Table 1, in order to identify optimal plating conditions. In this study the authors simply wished to single out the best operating conditions for the investigated bath and to characterise the coatings formed under such conditions: comprehensive electroanalytical or mechanistic studies of the electrodeposition process are beyond the scope of the present paper. Even

Table 1 Experimental parameters used for the electrodeposition of DLC coatings

Sample	Potential/V	Acetic acid vol%	Time/h	Temperature/°C
1	−8	1	1	room
2	−8	1	2	room
3	−8	1	5	room
4	−8	2	1	room
5	−8	5	1	room
6	−8	10	1	room
7	−15	1	1	room
8	−20	1	1	room

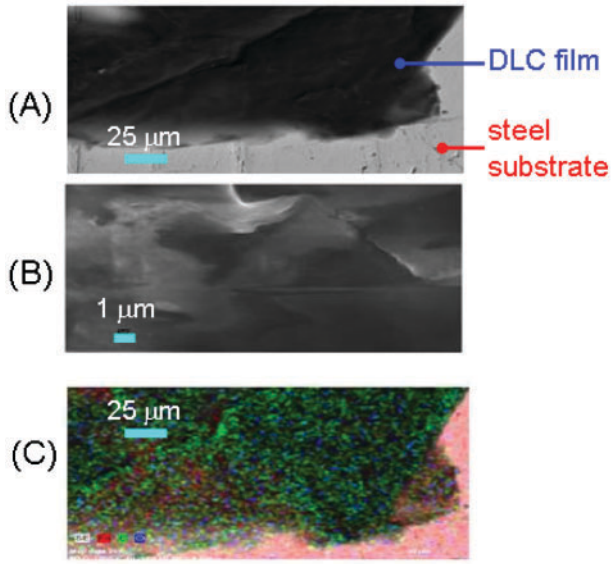

a The edge between the coating and the substrate (screened with a PTFE frame): scale bar 25 μm. *b* Detail of panel *a*: scale bar 1 μm. *c* Fe, C, O and elastic background *be* EDX maps of the region shown in panel *a*

1 SEM micrographs and EDS maps of a representative DLC coating on carbon steel, deposited at potential −8 V for 1 h from an aqueous solution with 1 vol% acetic acid

though in all the investigated growth conditions, uniform and continuous DLC films were grown, one particular condition appeared to be more convenient for the formation of high-quality coatings. A desirable effect for film quality is joule heating close to the cathode, favouring DLC formation for both kinetic (Arrhenius-type) and fluid-dynamic reasons (decrease in viscosity). The joule heating was controlled by adjusting the interelectrode diastance, the applied cell voltage and the bath conductivity and the effects of these changes in operating condition monitored by following the current circulating in the cell. With 1% acetic acid the reaction rate is too low, owing to the low concentration of reagent. By increasing the acetic acid percentage to 5–10%, the precursor concentration is sufficient to sustain the acceptable growth rate and conductivity of the electrolyte increases. Nevertheless, since the conductivity is positively correlated with acid content, 10% acetic acid causes an excessive decrease in joule heating, resulting in an insufficient activation of the reaction of the CH^{3+} group on the steel. Moreover, by increasing the percentage of acetic acid from 5 to 10%, the pH of the solution decreases in a way that favours the detachment of the DLC film.

Morphological and structural characterisation

The representative SEM micrographs are EDX maps shown in Fig. 1 which allow appreciation of the typical film morphology. Since the film is homogeneous on the mesoscopic scale, it is very difficult to image it under the microscope: in order to enhance the contrast, the authors chose to report SEM micrographs showing both the DLC film and the uncoated substrate (panels *a* and *c*), corresponding to the edge of the electrodeposit, close to the zone of the substrate that had been screened with the PTFE frame.

Raman spectroscopy was used to identify the chemical nature of the electrodeposited carbon-based films. In view of a quantitative compositional analysis, ten Raman spectra were measured in random locations of each sample and fitted with a Gaussian profile after background correction.[23] A selection of typical Raman spectra of an electrodeposited DLC film on steel are shown in Fig. 2, together with the corresponding peak deconvolution. The D-peak at 1363 cm^{-1} and the broad G-peak at 1558 cm^{-1} are diagnostic of a DLC film.[15–17,22,24] The G-peak at 1586 cm^{-1} is attributed to the graphite-like layers of sp^2 micro domains, while the D-peak at 1363 cm^{-1} corresponds to bond-angle disorder in the sp^2 graphite-like micro domains induced by the linking with sp^3-C atoms as well as the finite crystalline sizes of sp^2 micro domains. Moreover, the peak centred at 1489 cm^{-1} can be assigned to the asymmetrical deformation frequency of C–CH with sp^2 hybridised C–C bonding.[15–17] The intensity ratio between the D and G peaks (I_D/I_G) is a very diagnostic parameter for the evaluation of DLC-like materials. The literature reports that an increase in I_D/I_G ratio is correlated with an increase in the amount of sp^3 coordination.[25–28] Literature values of the I_D/I_G ratios for DLC coating obtained by different methods and under different conditions were found to vary in the interval 0·3–5 (see Table 3 for details). The I_D/I_G ratios were calculated for each measured point of a given sample and their averages are reported in Table 2. The data here reveal that I_D/I_G decreases from 3·03, for the films prepared at −8 V to 2·83 for those grown at −15 V, indicating that lower-quality films form at higher deposition voltages. Moreover, it was found that higher acetic acid concentrations give rise to larger I_D/I_G ratios.

Mechanical properties

Panels *a-c* of Fig. 3 show the microhardness of the DLC films as a function of potential, time and acetic acid concentration. The microhardness is negatively correlated with the applied potential; this behaviour, in turn, is related to the diamond-to-graphite ratio. In fact, in agreement with Wong *et al.*,[22] the hardness of DLC films is positively correlated with the Raman intensity ratio I_D/I_G. It can also be observed that by extending the deposition time a decrease in the microhardness occurs, that can be attributed to the tendency of the deposit to detach after 1 hour of electrodeposition. Moreover, from Fig. 3*c* one can notice a negative correlation between hardness and acetic acid concentration at higher concentrations. Optimal microhardness was found to correspond to the following processing parameters: potential −8 V, acetic acid concentration 5 vol%, 1 hour deposition time.

The adhesion of DLC films was estimated by scratch testing samples obtained in the experimental conditions listed in the Table 1. All samples exhibit a ductile failure mechanism, characterised by a series of nearly-circular micro-cracks, resulting from the tendency of the coating to conform to the scratch groove shape (Fig. 4). Micro-cracks depart from the scratching direction, according to the 'conformal cracking' pattern defined by ASTM C 1624. Even if all samples exhibit a ductile failure mechanism, the adhesion of DLC films shows a strong correlation with potential, deposition time and acetic acid concentration. Figures 3*d-i* show a weak

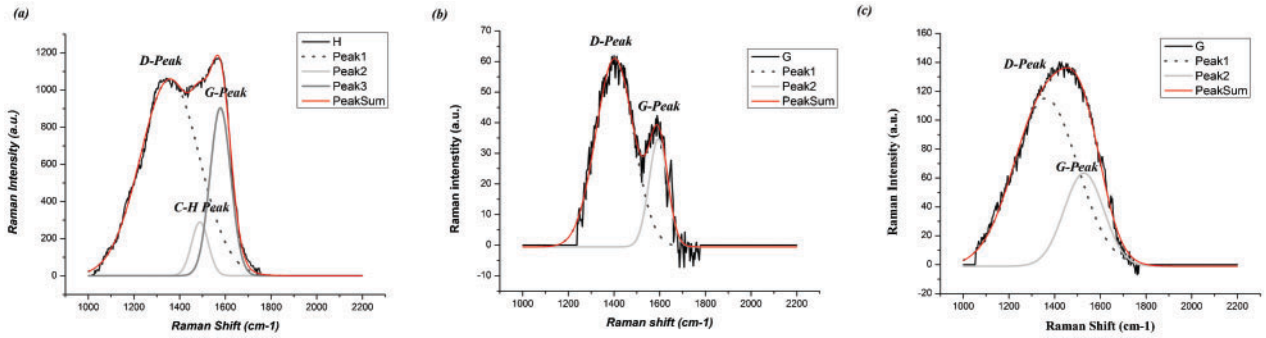

2 Representative Raman spectra of DLC films prepared by electrodepositing at: *a* −8 V for 1 h from a 1 vol% acetic acid bath; *b* −8 V for 1 h from a 5 vol% acetic acid bath; *c* −15 V for 1 h from a 1 vol% acetic acid bath

dependence of critical scratch loads (CSL: panels *d-f*) and coating shear stresses (CSS: panels *g-i*) on potential, deposition time and acetic acid content. Notwithstanding the fact that the variation range of the relevant mechanical parameters is rather limited and the measured error bars are relatively large, some correlations seem to appear with the operating conditions. In particular, it was found that CSL and CSS tend to: (i) decrease by increasing the potential; (ii) decrease with deposition time and (iii) increase by increasing the acetic acid concentration up to 5 vol% concentration, while they decrease for higher concentrations. The highest hardness and adhesion were found to correspond with the same processing parameters, that can thus be regarded as the optimal set for the relevant process: −8 V, 5 vol% acetic acid, 1 h deposition time. The thickness measurement of 5 replicate DLC films deposited under these conditions was performed by spectroellipsometry and averaged 272 ± 37 nm.

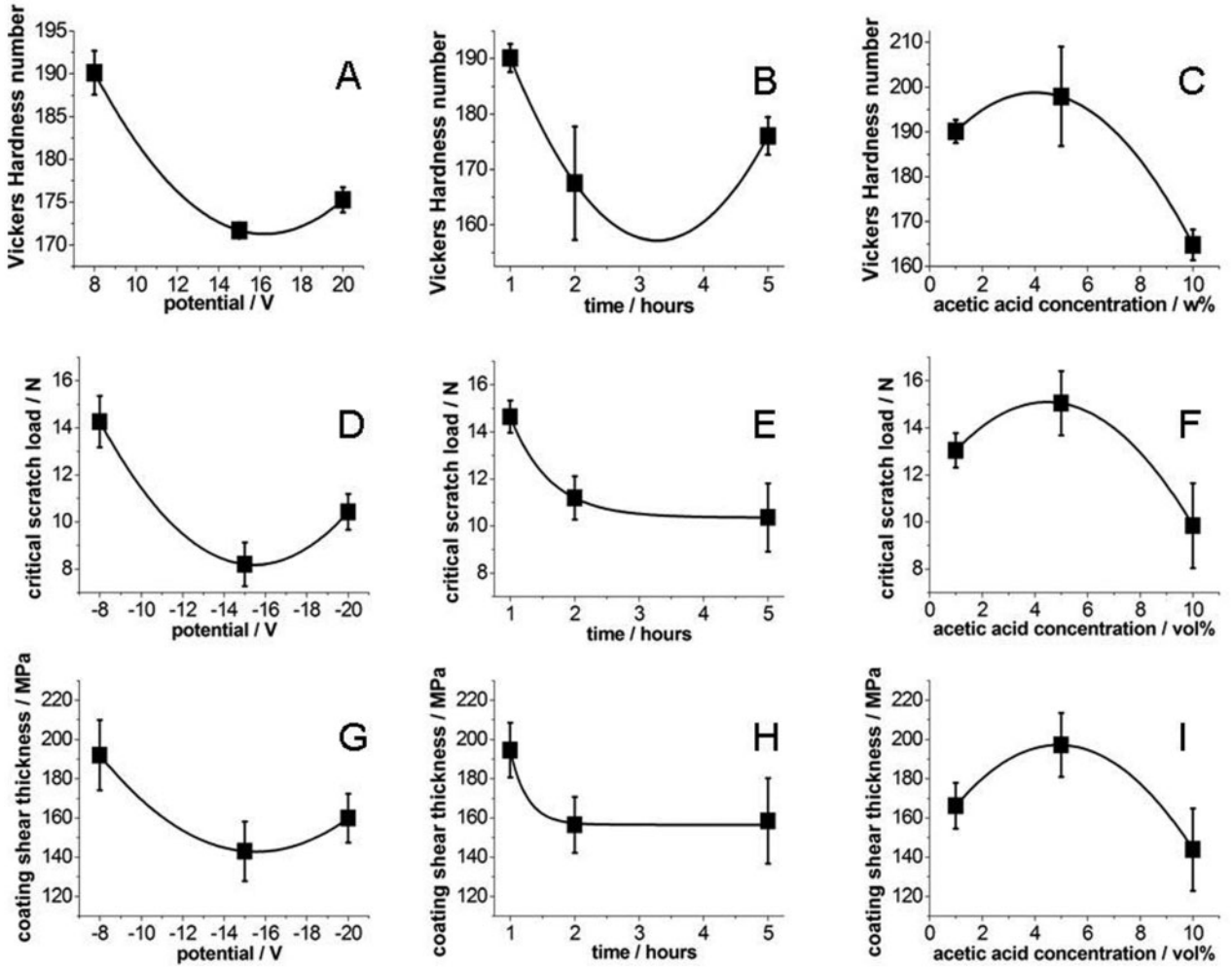

3 Effect of potential, time and acetic acid concentration on mechanical properties of DLC films on carbon steel (deposition conditions: potential −8 V, acetic acid concentration 5 vol%, time 1 h). *a–c* Microhardness; (D–I) adhesion expressed in terms of critical scratch load *d–f* and shear thickness *g–i*. The lines are a guide for the eye

Table 2 DLC electrodeposition parameters and corresponding diamond to graphite ratios (I_D/I_G), as evaluated by Raman spectroscopy

Sample	Potential/V	Acetic acid vol%	Time/h	I_D/I_G
1	−8	1	1	3·03±0·12
2	−8	5	1	3·32±0·12
3	−15	1	1	2·83±0·06

Corrosion resistance

In the literature, DLC coatings have not been primarily considered for their ability to impart protection against corrosion, in addition to the desired wear resistance. Nevertheless several studies have appeared on the enhancement of stainless steel corrosion performance by DLC coatings; a smaller number of papers have dealt with corrosion of DLC-coated Ti-base alloys and a limited amount of work, listed in the next paragraph, has been devoted to carbon-, low alloy- and tool-steels.

The studies on the protective effects of DLC coatings on carbon-, low alloy- and tool-steels have been based on exposure tests in a range of environments,[37,38] potentiodynamic measurements[39–41] and EIS.[41] In general, poor protection is reported, with no or limited improvement of the corrosion behaviour with respect to the uncoated steel. In the present research a *ca*. 270 nm thick coating grown under the optimal conditions defined in the previous Section has been tested. The corrosion tests were performed after one hour of immersion at open circuit potential by EIS again at open circuit potential. Only open-circuit conditions were considered, because the solution is rather aggressive to the substrate and applied anodic polarisation results in immediate failure of both uncoated and coated steel. In Fig. 5 EIS spectra for carbon steel without and with electrodeposited DLC coatings are compared. The EIS spectra can be modelled with RC parallel equivalent circuits, featuring a faradaic resistance R and a double-layer capacitance C. The experimental data can be approximately followed with a single RC parallel – representing a corrosion mechanism implying just one dominating faradaic reaction (fitting results depicted with the dotted, grey lines) – but can be better followed with the series of two RC parallels, denoting the fact that the corrosion mechanism entails

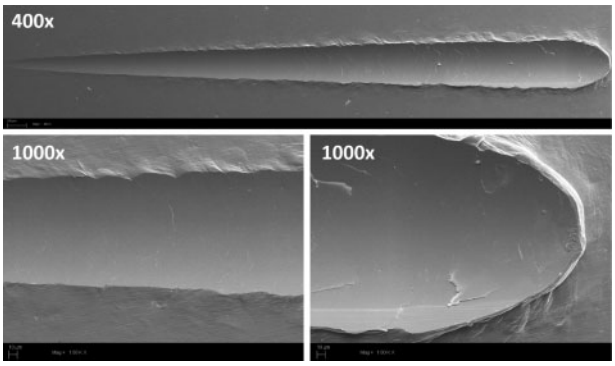

4 SEM micrographs illustrating a typical result of the scratch-testing of DLC-coated steel (deposition conditions: potential −8 V, acetic acid concentration 5 vol%, time 1 h)

two successive faradaic steps. More mechanistic details are beyond the scope of the present paper, which is focussed on the functional behaviour of electrodeposited DLC coatings. Specimens without and with DLC films exhibit total faradaic resistances R_1+R_2 of 341±17 and 543±31 Ω cm^2, respectively, denoting a limited, but measurable degree of corrosion protection, essentially imparted by the sound continuity of the DLC film. Moreover, the distortion from the circular shape observed at low frequencies for the uncoated sample denotes a progressive activation of the corrosion process,[42] that is absent in the coated one: this is a further indication of a slightly improved environmental stability.

Conclusions

Electrodeposition of high-quality DLC onto carbon steel from aqueous acetate solutions is described in this paper. Applying cell voltages in the range from −8 to −20 V between a steel cathode and a graphite anode in aqueous solution containing from 1 to 10 vol% of acetic acid for 1–5 hours, DLC films form with different contents of diamond *vs*. graphite carbon coordination, as assessed by quantitative Raman spectroscopy. The chemical quality of DLC was found to decrease with applied potential and to exhibit a maximum with respect to acetate concentration. In agreement with the

Table 3 Literature values of the Raman diamond to graphite ratios (I_D/I_G) for DLC films obtained by different methods

Literature methods for the deposition of DLC films	I_D/I_G	References
Electrodeposition	0·6–0·8	[29]
Electrodeposition	0·8–0·9	[30]
Electrodeposition	1·1–1·2	[31]
Electrodeposition	0·6–1	[12]
Electrodeposition	1·5–1·7	[32]
Electrodeposition	0·9–1·4	[33]
Pulsed laser deposition	0·5–0·8	[10]
Electrodeposition	0·9	[34]
Electrodeposition	0·8–1	[13]
KrF pulsed laser deposition	0·3–0·7	[35]
Unbalanced d.c. magnetron sputtering	3–5	[22]
Electrodeposition	1·96–1·84	[17]
ECR-CVD	0·4–0·8	[8]
Plasma CVD	0·7	[9]
Magnetic field enhanced plasma deposition (MEPD)	1–4	[21]
PECVD	0·3–0·4	[7]
Plasma immersion ion implantation-deposition	0·5–1·6	[36]
Electrodeposition	1·72–1·74	[14]

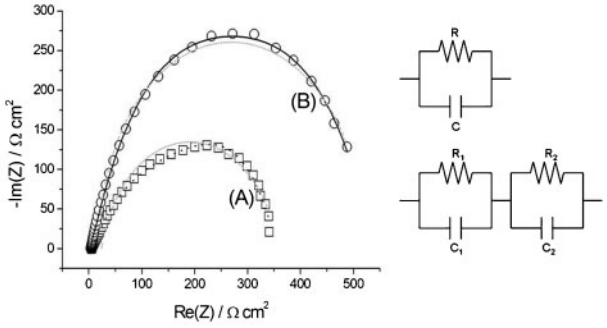

5 Left: Electrochemical impedance spectra for: *a* uncoated and *b* DLC-coated steel samples. DLC grown at −8 V from 5 vol% acetic acid bath for 1 h. Test solution: aerated 0·8 M NaCl aqueous solution. Test conditions: open circuit potential, 10 mV amplitude, 65 kHz–10 mHz frequency span. Right: equivalent circuit models. Symbols: experimental data; solid lines: fitting with two-RC parallel model; dotted, grey lines: fitting with one-RC parallel model

literature, the hardness of the films correlates positively with the amount of sp^3 coordination. Notably, all samples studied in this research - regardless of the relative DLC quality - exhibit a ductile failure mechanism in scratch tests. Film adhesion is strongly dependent on processing conditions: it is negatively correlated with potential and electrodeposition time and it exhibits a maximum for an acetic acid concentration of 5 vol%. Optimal microhardness and adhesion were thus found to correspond with the following processing conditions: cell voltage −8 V, acetic acid concentration 5 vol%, deposition time 1 hour, at which films of *ca*. 270 nm form. Electrochemical impedance measurements at open circuit potential in aerated 0·8 M NaCl solutions show that the films formed under optimal conditions exhibit a slight protective effect with respect to corrosion, by increasing the polarisation resistance by a factor of *ca*. 1·5.

References

1. H. Buchkremer-Hermanns, H. Ren and H. Wei: *Surf. Coat. Technol.*, 1995, **74**, 215–220.
2. A. Dehbi-Alaoui and A. Matthews: *Vacuum*, 1995, **46**, 1305–1309.
3. K. Kuramoto, Y. Domoto, H. Hirano, S. Kiyama and S. Tsuda: *Appl. Surf. Sci.*, 1997, **113**, 227–230.
4. D. S. Patil, K. Ramachandran, N. Venkatramani, M. Pandey, S. Venkateswaran and R. D'Cunha: *J. Alloys Compd.*, 1998, **278**, 130–134.
5. C. Meunier, E. Tomasella, S. Vives and S. Mikhailov: *Diam. Relat. Mater.*, 2001, **10**, 1491–1496.
6. M. Ban, M. Ryoji, T. Hasegawa, Y. Mori, S. Fujii and J. Fujjoka: *Diam. Relat. Mater.*, 2002, **11**, 1353–1359.
7. K. Navaneetha Pandiyaraj, V. Selvarajan, J. Heeg, F. Junge, A. Lampka, T. Barfels, M. Wienecke, Y. Ha Rhee and H. Woo Kim: *Diam. Relat. Mater.*, 2010, **19**, 1085–1092.
8. A. Pardo and C. Gómez-Aleixandre: *Vacuum*, 2011, **85**, 1140–1143.
9. R. Paul, S. Hussain and A. K. Pal: *Appl. Surf. Sci.*, 2009, **255**, 8076–8083.
10. A. Usman, M. S. Rafique, M. Khaleeq-ur-Rahman, K. Siraj, Safia Anjum, H. Latif, Taj M. Khan and M. Mehmood: *Mater. Chem. Phys.*, 2011, **126**, 649–654.
11. Y. Namba: *J. Vac. Sci. Technol.*, 1992, **A 10**, 3368–3370.
12. H. Pang, X. Wang, G. Zhang, H. Chen, G. Lv and S. Yang: *Appl. Surf. Sci.*, 2010, **256**, 6403–6407.
13. S. Gupta, M. Pal Chowdhury and A. K. Pal: *Diam. Relat. Mater.*, 2004, **13**, 1680– 1689.
14. R. K. Roy, B. Deb, B. Bhattacharjee and A. K. Pal: *Thin Solid Films*, 2002, **422**, 92–97.
15. S. Gupta, R. K. Roy, B. Deb, S. Kundu and A. K. Pal: *Mater. Lett.*, 2003, **57**, 3479– 3485.
16. S. Wan, H. Hu, G. Chen and J. Zhang: *Electrochem. Comm.*, 2008, **10**, 461–465.
17. K. Sreejith, J. Nuwad and C. G. S. Pillai: *Appl. Surf. Sci.*, 2005, **252**, 296–302.
18. WenLiang He, Rui Yu, Hao Wang and Hui Yan: *Carbon*, 2005, **43**, 2000–2006.
19. T. Paulmier, J. M. Bell and P. M. Fredericks: *Thin Solid Films*, 2007, **515**, 2926–2934.
20. B. Bozzini, M. Boniardi. *J. Mater. Sci.*, 2001, **36**, 511–518.
21. J. Schwan, S. Ulrich, V. Batori, H. Ehrhardt, and S. R. P. Silva: *J. Appl. Phys.*, 1996, **80**, 440–447.
22. P. L. Wong, F. He and X. Zhou: *Tribology International*, 2010, **43**, 1806–1810,
23. B. Bozzini, L. D'Urzo and C. Mele: *J. Electrochem. Soc.*, 2005, **152**, C255–C264.
24. K. Ma, G. Yang, L. Yu and P. Zhang: *Surf. Coat. Technol.*, 2010, **204**, 2546–2550.
25. H. Wang, M. R. Sheng, Z. Y. Ning, C. Ye, H. Y. Dan, C. C. Cao and H. S. Zhu: *Thin Solid Films*, 1997, **293**, 87–90.
26. T. W. Scharf, H. Deng and J. A. Barnard: *J. Appl. Phys.*, 1997, **81**, 5393–5395.
27. H. Pang, X. Wang, G. Zhang, H. Chen, G. Lv and S. Yang: *Appl. Surf. Sci.*, 2010, **256**, 6403–6407.
28. P. L. Wong, F. He and X. Zhou: *Tribology International*, 2010, **43**, 1806–1810.
29. S. C. Ray, B. Bose, J. W. Chiou, H. M. Tsai, J. C. Jan, Krishna Kumar, W. F. Pong, D. Gupta, G. Fanchini and A. Tagliaferro: *J. Mater. Res.*, 2004, **19**, 1126–1132.
30. D. Huang, S. Wan, L. Wang, and Q. Xue: *Surf. Interface Anal.*, 2011, **43**, 1064–1068.
31. S. Wan, L. Wang and Q. Xue: *Electrochem. Comm.*, 2009, **11**, 99–102.
32. S. Wan, L. Wang and Q. Xue: *Electrochem. Comm.*, 2010, **12**, 61–65.
33. S. Wan, L. Wang and Q. Xue: *Appl. Surf. Sci.*, 2011, **257**, 10000–10004.
34. R. Paul, S. Dalui, S. N. Das, R. Bhar and A. K. Pal: *Appl. Surf. Sci.*, 2008, **255**, 1705–1711.
35. H. Wong, Y. M. Foong and D. H. C. Chua: *Appl. Surf. Sci.*, 2011, **257**, 9616–9620.
36. J. Y. Chen, L. P. Wang, K. Y. Fu, N. Huang, Y. Leng, Y. X. Leng, P. Yang, J. Wang, G. J. Wan, H. Sun, X. B. Tian and P. K. Chu: *Surf. Coat. Technol.*, 2002, **156**, 289–294.
37. P. Couvrat, M. Denis, M. Langer, S. Mitura, P. Niedzielsk and J. Marciniak: *Diam. Relat. Mater.*, 1995, **4**, 1251–1254
38. G. Thorwarth, C. Hammerl, M. Kuhn, W. Assmann, B. Schey and B. Stritzker: *Surf. Coat. Technol.*, 2005, **193**, 206– 212.
39. J. Kaminski, J. Rudnicki, T, C. Nouveau, A. Savan and P. Beer: *Surf. Coat. Technol.*, 2005, **200**, 83–86.
40. G. Reisel, G. Irmer, B. Wielage and A. Dorner-Reisel: *Thin Solid Films*, 2006, **515**, 1038–1042.
41. R. P. O. S. Nery, R. S. Bonelli and S. S. Camargo Jr.: *J. Mater. Sci.*, 2010, **45**, 5472–5477.
42. B. Bozzini, G. P. De Gaudenzi and C. Mele: *Corr. Eng. Sci. Technol.*, 2005, **40**, 290–300.